model and $P = 0.08$ for the second-order term, β_2, suggesting a trend for an inverted-u shape; D2: linear $r^2 = 0.11$, $P = 0.26$; quadratic $r^2 = 0.12$, $P = 0.53$). Next we investigated the effect of training. For each participant, D1 BP change was averaged across the five ROIs. The change in WM capacity could be explained by both the linear model (negative correlation, $P = 0.016$) and the quadratic model ($P = 0.001$). However, the quadratic model $\{WM_2 - WM_1 = [\alpha + \beta_1 BP_2 + \beta_2(BP_2)^2] - [\alpha + \beta_1 BP_1 + \beta_2(BP_1)^2]$, where WM_1 and WM_2 represent WM capacity before and after training, respectively; and BP_1 and BP_2 represent BP before and after training, respectively$\}$ predicted a larger amount of variance ($r^2 = 0.75$) as compared to the linear model ($r^2 = 0.42$; r^2 of change between models = 0.33, $P = 0.005$). The quadratic model was then fitted for each region individually and described the data at a statistically significant level ($P < 0.05$) for the right ventrolateral frontal, right dorsolateral frontal, and both posterior ROIs (Fig. 2, F to J). For D2 BP, the average change across all ROIs was not related to the change in WM capacity (linear model: $r^2 = 0.02$, $P = 0.67$; quadratic model: $r^2 = 0.08$, $P = 0.66$).

These findings show that training-related changes in WM capacity are associated with changes in D1 BP. The binding of [^{11}C]SCH23390 has been shown to be insensitive to the immediate effect of drugs changing endogenous dopamine concentration and may thus serve as an index for the density of available D1 receptors (*25*). Although the relation between performance and dopamine BP is probably nonlinear, our data (Fig. 2, F to J) generally showed that, within the measured range, a negative correlation dominated for all regions, with larger decreases in D1 BP being associated with larger improvements in WM. This is consistent with the finding that low doses of a D1 antagonist enhance the delay activity of prefrontal neurons during the performance of WM tasks (*18*, *19*). An association between a decrease in BP and an increase in WM is also consistent with the negative correlation observed between WM capacity and D1 binding in individuals with schizophrenia (*26*).

The underlying mechanisms responsible for the plasticity of receptor densities are not known. One possibility is that other transmitters influence the trafficking of dopamine receptors; for example, it has been shown that the activation of *N*-methyl-D-aspartate receptors affects dopamine signaling by recruiting D1 receptors from the interior of the cell to the plasma membrane (*27*). Another interpretation is that the changes reflect long-term adjustment of the concentration of D1 receptors in response to a prolonged increase in the level of endogenous dopamine during WM training.

More generally, the present results demonstrate a high level of plasticity of the neuronal system defined by cortical D1 receptors in human volunteers. The findings were specific because the D2 system did not show any relation to WM changes. The training-induced changes emphasize the reciprocal interplay between behavior and the underlying brain biochemistry and should be relevant for studies of neuropsychiatric disorders as well as correlational studies between behavior and biochemical markers.

References and Notes

1. H.-M. Süß, K. Oberauer, W. W. Wittmann, O. Wilhelm, R. Schulze, *Intelligence* **30**, 261 (2002).
2. A. Baddeley, *Nat. Rev. Neurosci.* **4**, 829 (2003).
3. P. S. Goldman-Rakic, *J. Neuropsychiatry Clin. Neurosci.* **6**, 348 (1994).
4. F. X. Castellanos, R. Tannock, *Nat. Rev. Neurosci.* **3**, 617 (2002).
5. K. L. Bopp, P. Verhaeghen, *J. Gerontol. B Psychol. Sci. Soc. Sci.* **60**, 223 (2005).
6. J. M. Swanson *et al.*, *Neuropsychol. Rev.* **17**, 39 (2007).
7. M. Laruelle, *Q. J. Nucl. Med.* **42**, 211 (1998).
8. T. Klingberg, H. Forssberg, H. Westerberg, *J. Clin. Exp. Neuropsychol.* **24**, 781 (2002).
9. P. Olesen, H. Westerberg, T. Klingberg, *Nat. Neurosci.* **7**, 75 (2004).
10. T. Klingberg *et al.*, *J. Am. Acad. Child Adolesc. Psychiatry* **44**, 177 (2005).
11. S. M. Jaeggi, M. Buschkuehl, J. Jonides, W. J. Perrig, *Proc. Natl. Acad. Sci. U.S.A.* **105**, 6829 (2008).
12. E. Dahlin, A. S. Neely, A. Larsson, L. Bäckman, L. Nyberg, *Science* **320**, 1510 (2008).
13. T. J. Brozoski, R. M. Brown, H. E. Rosvold, P. S. Goldman, *Science* **205**, 929 (1979).
14. U. Müller, D. Y. von Cramon, S. Pollmann, *J. Neurosci.* **18**, 2720 (1998).
15. T. Sawaguchi, P. S. Goldman-Rakic, *Science* **251**, 947 (1991).
16. T. Sawaguchi, P. S. Goldman-Rakic, *J. Neurophysiol.* **71**, 515 (1994).
17. S. Aalto, A. Brück, M. Laine, K. Någren, J. O. Rinne, *J. Neurosci.* **25**, 2471 (2005).
18. G. V. Williams, P. S. Goldman-Rakic, *Nature* **376**, 572 (1995).
19. S. Vijayraghavan, M. Wang, S. G. Birnbaum, G. V. Williams, A. F. Arnsten, *Nat. Neurosci.* **10**, 376 (2007).
20. M. S. Lidow, G. V. Williams, P. S. Goldman-Rakic, *Trends Pharmacol. Sci.* **19**, 136 (1998).
21. J. X. Cai, A. F. Arnsten, *J. Pharmacol. Exp. Ther.* **283**, 183 (1997).
22. H. Brismar, M. Asghar, R. M. Carey, P. Greengard, A. Aperia, *Proc. Natl. Acad. Sci. U.S.A.* **95**, 5573 (1998).
23. M. Soiza-Reilly, M. Fossati, G. R. Ibarra, J. M. Azcurra, *Brain Res.* **1004**, 217 (2004).
24. B. R. Postle, M. D'Esposito, *J. Cogn. Neurosci.* **11**, 585 (1999).
25. N. Guo *et al.*, *Neuropsychopharmacology* **28**, 1703 (2003).
26. A. Abi-Dargham *et al.*, *J. Neurosci.* **22**, 3708 (2002).
27. L. Scott *et al.*, *Proc. Natl. Acad. Sci. U.S.A.* **99**, 1661 (2002).

28. The authors thank C. Halldin, K. Kolaas, G. Lei, J. Macoveanu, and members of the Karolinska Institutet PET center for assistance in the PET measurements. This work was supported by the Swedish Foundation for Strategic Research, Swedish Research Council, VINNOVA (the Swedish Governmental Agency for Innovation Systems), and Knut and Alice Wallenberg Foundation.

Supporting Online Material

www.sciencemag.org/cgi/content/full/323/5915/800/DC1
Methods
Table S1
References

18 September 2008; accepted 10 December 2008
10.1126/science.1166102

Axon Regeneration Requires a Conserved MAP Kinase Pathway

Marc Hammarlund,[1,2]*† Paola Nix,[1]† Linda Hauth,[1] Erik M. Jorgensen,[1,2] Michael Bastiani[1]‡

Regeneration of injured neurons can restore function, but most neurons regenerate poorly or not at all. The failure to regenerate in some cases is due to a lack of activation of cell-intrinsic regeneration pathways. These pathways might be targeted for the development of therapies that can restore neuron function after injury or disease. Here, we show that the DLK-1 mitogen-activated protein (MAP) kinase pathway is essential for regeneration in *Caenorhabditis elegans* motor neurons. Loss of this pathway eliminates regeneration, whereas activating it improves regeneration. Further, these proteins also regulate the later step of growth cone migration. We conclude that after axon injury, activation of this MAP kinase cascade is required to switch the mature neuron from an aplastic state to a state capable of growth.

Severed neurons can regenerate. After axons are cut, neurons can extend a new growth cone from the axon stump and can attempt to regrow a normal process. Most invertebrate neurons are able to regenerate, as are neurons in the mammalian peripheral nervous system. By contrast, neurons in the mammalian central nervous system have limited regenerative capability (*1*). Regeneration is thought to be initiated by signals arising from the injury, including calcium spikes and the retrograde transport and nuclear import of regeneration factors (*2*). These mechanisms lead to increased cyclic adenosine monophosphate (cAMP) levels, local and somatic protein synthesis, and changes in gene transcription that, in turn, promote remodeling of the cytoskeleton and plasma membrane at the site of injury. The ability of specific neurons to regenerate is deter-

[1]Department of Biology, University of Utah, 257 South 1400 East, Salt Lake City, UT 84112–0840, USA. [2]Howard Hughes Medical Institute, University of Utah, 257 South 1400 East, Salt Lake City, UT 84112–0840, USA.

*Present address: Department of Genetics and Program in Cellular Neuroscience, Neurodegeneration and Repair, Yale University School of Medicine, 295 Congress Avenue, New Haven, CT 06510, USA.
†These authors contributed equally to this work.
‡To whom correspondence should be addressed. E-mail: bastiani@bioscience.utah.edu

mined in part by the balance between proregeneration signals and cellular pathways that inhibit regeneration. For example, regeneration in the mammalian CNS is inhibited by extrinsic signals from myelin and chondroitin sulfate proteoglycans; these signals activate pathways in the damaged neuron that prevent regrowth (*3*). But CNS regeneration can be achieved even in the presence of inhibitory signals. A conditioning lesion to a peripheral process results in increased regeneration of the CNS branch of dorsal root ganglion neurons, presumably by triggering injury signals that result in an overall increase in regenerative potential (*4*). Thus, intrinsic regeneration signals can influence regenerative success, and these signaling processes represent potential targets for therapies to enhance regeneration.

We identified the mitogen-activated protein (MAP) kinase kinase kinase (MAPKKK) *dlk-1* as essential for regeneration in the course of a large screen for genes required for regeneration. This screen was conducted in a β-spectrin mutant (*unc-70*) background (*5*). Neurons in β-spectrin mutant nematodes break because of mechanical strain induced by locomotion. The γ-aminobutyric acid (GABA)–releasing motor neurons respond to breaks by regenerating toward their targets in the dorsal cord (*6*). Axon guidance during regeneration is imperfect, resulting in axons in mature animals with branching and other abnormalities (Fig. 1). We found that RNA interference of *dlk-1* eliminates regeneration in *unc-70* mutant animals. Neither *unc-70* (*6*) nor *dlk-1* (*7*) is essential for axon outgrowth during development of the GABA neurons (Fig. 1) (*8*). The *unc-70 dlk-1* synthetic phenotype for axon morphology suggests that *dlk-1* may function specifically in regeneration.

To demonstrate that *dlk-1* functions in regeneration independently of *unc-70*, we used laser axotomy to trigger regeneration. The GABA motor neurons can regenerate after laser axotomy (*9*). We used a pulsed 440-nm laser to cut axons (*10*). In larval stage 4 (L4) wild-type animals, 70% of severed axons initiated growth cones within 24 hours after axotomy (Fig. 2 and table S1). But when axons were cut in L4 stage *dlk-1(ju476)* null mutants, growth cones were never observed. These severed neurons appeared healthy after surgery; both the stump of the remaining axon and its cell body showed no decrease in green fluorescent protein (GFP) expression or other signs of injury. Nevertheless, these neurons failed to regenerate. To test whether regeneration was merely delayed, we monitored some severed axons for 5 days; regeneration still was not observed. Thus, *dlk-1* is essential for axon regeneration after spontaneous breaks and after laser surgery but is dispensable for axon outgrowth during development.

Mosaic experiments demonstrate that the DLK-1 protein acts in the damaged cell rather than in the surrounding tissue. To determine whether DLK-1 acts cell-autonomously to promote regeneration, we expressed *dlk-1* under the GABA-specific promoter P*unc-47* in the *dlk-1* null background. Neurons were severed by laser surgery, and regeneration was assayed after 18 to 24 hours. We found that expressing DLK-1 in the GABA neurons restored regeneration to *dlk-1* null mutants (Fig. 2C). Further, mutations that affect DLK-1 levels also affect regeneration (Fig. 2D). In *Caenorhabditis elegans*, DLK-1 levels are negatively regulated by RPM-1 (*7*). Overexpression of RPM-1 reduced regeneration after surgery to levels similar to those of *dlk-1* loss-of-function mutants. Conversely, initiation of regeneration was enhanced in *rpm-1* mutant animals. Initiation of regeneration was also enhanced in animals lacking FSN-1, an F-box protein that functions with RPM-1 to promote DLK-1 degradation (*11*). However, loss of GLO-1 (Rab) or GLO-4 (Rab guanine nucleotide exchange factor), both of which mediate ubiquitin-independent functions of RPM-1 (*11*), did not have strong effects on regeneration. These results confirm that changes in DLK-1 protein abundance can determine regenerative ability.

Although regeneration is age-dependent, *dlk-1* is required at all stages, and overexpression of DLK-1 can rescue some age-dependent decline (Fig. 2E). We analyzed regeneration at various developmental stages. We found that regeneration declines significantly with age, and only a few axons in old adults regenerated (*10*). Despite these differences, *dlk-1* is required for all regeneration, even in very young animals. Because growth cones in the very young animals had not yet reached their targets, the dependence on *dlk-1* is not correlated with target contact or synaptogenesis. Further, *dlk-1* is required for regeneration of both presynaptic and postsynaptic processes (*8*).

To mediate regeneration, DLK-1 is required at the time of injury (Fig. 2F). We expressed the DLK-1 protein at different times using the heat shock promoter *Phsp-16.2*. DLK-1 expression at the time of injury was sufficient for regeneration. Applying heat shock hours before or hours after surgery resulted in less regeneration, and when heat shock was applied either 11 hours before or 48 hours after surgery, little or no regeneration was observed. This effect was independent of age, because surgery in L2 stage larvae failed to elicit regeneration when heat shock was applied 48 hours later. Thus, DLK-1 must function within a short temporal window near the time of injury to mediate regeneration, rather than establishing a permissive state for regeneration during development. These data suggest that DLK-1 signaling must coincide with other proregeneration signals, such as calpain activation (*12*) or cAMP elevation (*13*–*15*), for regeneration to occur.

DLK-1 is required for growth cone formation rather than the earlier step of filopodial extension. We used time-lapse microscopy to monitor morphological changes in axons after surgery. We

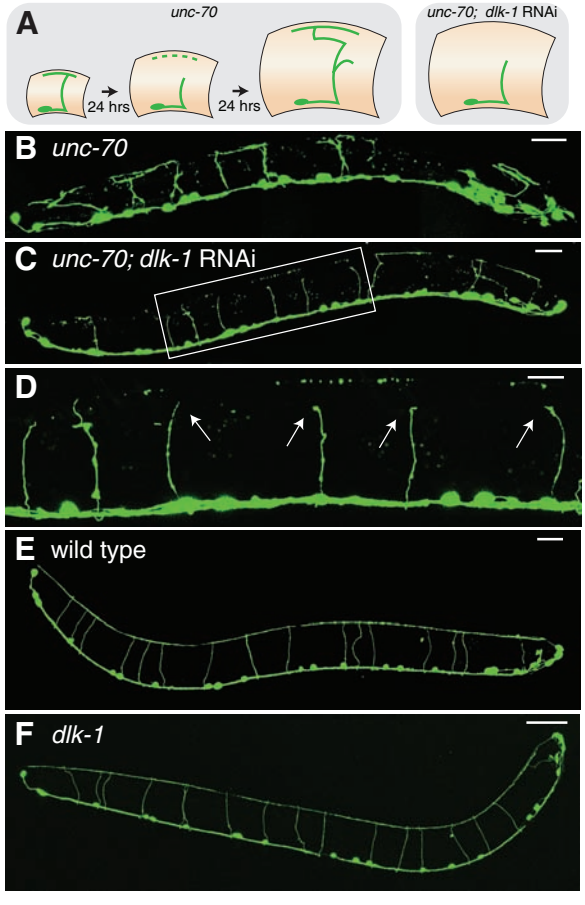

Fig. 1. *dlk-1* is required for axon regeneration in β-spectrin mutant nematodes. (**A**) Cartoon showing development of axon morphology in control β-spectrin mutant (left) and in β-spectrin mutant lacking hypothetical regeneration gene, e.g., *dlk-1* (right). (**B** and **C**) GABA neurons in representative L4 stage β-spectrin mutants (*unc-70*), expressing green fluorescent protein, under control conditions or after *dlk-1* RNA interference. Scale bars, 20 μm. (**D**) High-magnification view of boxed region in (C). Arrows indicate inert axon stumps. Scale bar, 10 μm. (**E** and **F**) GABA neurons in representative L4 stage wild-type and *dlk-1* mutant animals. Scale bars, 20 μm.

found that in wild-type animals, newly severed axons repeatedly extend short, transient filopodia from the axon stump (Fig. 3 and movie S1). The first filopodium appears with an average delay of more than 3 hours. In animals that successfully initiate regeneration, a single filopodium eventually persists and is transformed into a growth cone. Growth cone formation in wild-type animals occurs with an average delay of 7 hours after surgery. In *dlk-1* mutants, transient filopodia appear at approximately the same time and the same rate as in the wild type. However, growth cones were never observed in these mutants. These data demonstrate that DLK-1 is required to transform exploratory filopodia into growth cones.

Increased expression of DLK-1 in wild-type animals accelerates the formation of growth cones and improves migration success. We overexpressed DLK-1 in GABA neurons and found that time of growth cone initiation by axon stumps was advanced relative to the wild type (Fig. 3 and movie S1). Also, more axons initiated growth cones (Fig. 4). In addition to these effects on growth cone initiation, DLK-1 overexpression improved growth cone performance. In wild-type animals, regenerating growth cones often have a branched, dystrophic morphology. Dystrophic growth cones migrate poorly, and most never reach the dorsal nerve cord in 24 hours (Fig. 3). These dystrophic growth cones resemble dystrophic growth cones observed in failed regeneration in the mammalian CNS (*16*). By contrast, regenerating growth cones in neurons that overexpress DLK-1 have a compact shape, similar to growth cones observed during initial axon development (*17*). These compact growth cones were much more likely to reach the dorsal nerve cord. Growth cone migration during regeneration in *C. elegans* shares some genetic requirements with developmental axon guidance, including components of the netrin and slit signaling pathways (*18*) and the ephrin pathway (*10*). It is possible that DLK-1 overexpression improves regeneration by affecting the response of the growth cone to such signals. Thus, DLK-1 acts at two steps of regeneration: It is required for growth cone formation, and it also controls growth cone morphology and behavior.

DLK-1 functions in a MAP kinase signaling cascade that also includes the MAP kinase kinase (MAPKK) MKK-4, and the p38 MAP kinase PMK-3 (*7*). We tested whether this entire MAP kinase signaling module functions in regeneration by examining null mutants in *mkk-4* and *pmk-3*. Like *dlk-1*, neither of these mutants has appreciable defects in axon outgrowth during development. But after axotomy, both mutant strains fail to initiate regeneration (Fig. 4A). These data suggest that MKK-4 and PMK-3 are the downstream targets of DLK-1 for regeneration. Inhibition of p38 also reduces regeneration of cultured vertebrate neurons (*19*), which suggests that the function of p38 MAP kinases in regeneration is conserved. Do other MAP kinase cascades also contribute to regeneration? We tested a sampling of *C. elegans* MAP kinase components and found that mutations in these genes did not eliminate regeneration (Fig. 4B and table S1). Initiation of regeneration was not affected by loss of the MAPKKK *nsy-1* or its target MAPKK *sek-1*. Loss of the MAPKK *jkk-1* also did not affect regeneration. By contrast, loss of the MAPKKK *mlk-1* reduced initiation of regeneration (although some regeneration still occurred), as did loss of its downstream target *mek-1*. MLK-1 and MEK-1 are thought to activate a second *C. elegans* p38 MAP kinase, PMK-1 (*20*), which suggests that multiple p38 family members contribute to regeneration. (Because null mutations in *pmk-1* are lethal, we were unable to test its function directly.) Loss of the MAP kinase *jnk-1* increased initiation of regeneration. Thus, whereas the DLK-1/MKK-4/PMK-3 MAP kinase cascade is required to initiate regeneration, other MAP kinase pathways also regulate this process. Consistent with these data, mutations in *mkk-4* or *pmk-3* did not eliminate the stimulation of regeneration by DLK-1 overexpression, which suggests that cross-talk between MAP kinase modules may contribute to regeneration (Fig. 4C). However, the modest phenotype of other MAP kinase mutants and the inability of DLK-1 overexpression to bypass the requirement for *mkk-4* and *pmk-3* suggest that the DLK-1/MKK-4/PMK-3 module is the major MAP kinase pathway for axon regeneration.

What stimulates DLK-1 function when an axon breaks? In the simplest model, the axon break interrupts trafficking of DLK-1. Local DLK-1 accumulation in the injured neuron then leads to homodimerization and activation, followed by activation of the downstream targets MKK-4 and PMK-3 (Fig. 4D). Alternatively,

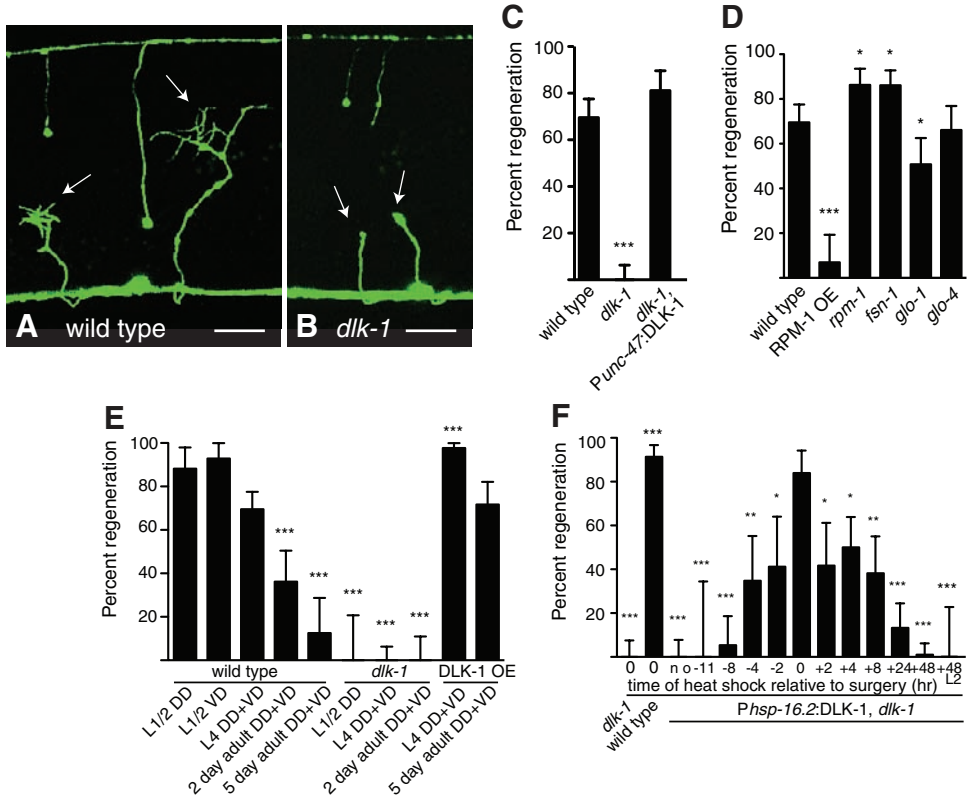

Fig. 2. *dlk-1* is required in severed axons for growth cone initiation. (**A**) Regenerating axons 18 to 20 hours after laser surgery in a wild-type animal. Both severed axons have generated a growth cone (arrows). Scale bar, 10 μm. (**B**) Axons in *dlk-1* mutants fail to generate growth cones 18 to 24 hours after surgery. Scale bar, 10 μm. (**C**) DLK-1 acts cell intrinsically to mediate regeneration. (**D**) RPM-1 controls DLK-1 activity in axon regeneration. (**E**) Regeneration requires *dlk-1* at all ages and overexpression of DLK-1 rescues age-associated decline. DD and VD are motor neurons of different lineages (*8*). (**F**) DLK-1 acts at the time of injury to mediate regeneration. Time of heat shock relative to surgery is indicated in hours. No heat shock is indicated by "no." "L2" indicates surgery at the L2 stage. Axotomy at L4 stage unless indicated otherwise. (C) to (F) Percentage of axons that initiated regeneration and 95% confidence interval (CI). $*P < 0.05$, $**P < 0.01$, $***P < 0.001$.

specific regulatory mechanisms activate DLK-1 after injury, such as scaffolding proteins like Jip1 (*21*); phosphatases such as PP1, PP2a, and calcineurin (*22*); or regulators of the proteasome (*23*). The strict requirement for the DLK-1 pathway in regeneration suggests that mature neurons have intrinsic barriers to growth that are not present during development. Once axons have reached their target and have begun synaptogenesis, termination of growth signals by mechanisms like RPM-1 may down-regulate growth to allow synapse maturation and to stabilize neuronal architecture. Indeed, mutations in RPM-1 or its homologs cause overgrowth of axons in worms (*24*), aberrant sprouting in *Drosophila* (*25*), and aberrant growth cone initiation on axon shafts in mouse (*26*). We found that *dlk-1* is required for regeneration even in neurons that are actively growing at the time of injury. Further, overexpressing DLK-1 partially prevented the loss of regeneration in old animals (Fig. 2E). Thus, barriers to growth are quickly erected in axons, and post-injury signaling via DLK-1, MKK-4, and PMK-3 is required to drive the neuron back to its prelapsarian, embryonic state.

How does the MAP kinase PMK-3 stimulate regeneration? The DLK-1 pathway is first required for growth cone formation about 7 hours after a break occurs—a process likely to be mediated by the polymerization of microtubules. Activated p38 MAP kinase regulates microtubule dynamics (*26*), and microtubule remodeling is required for growth cone initiation during regeneration (*27*). Further,

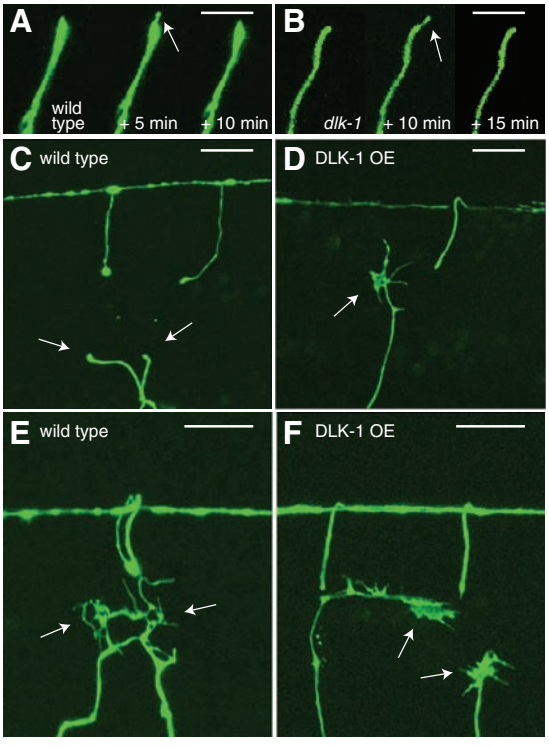

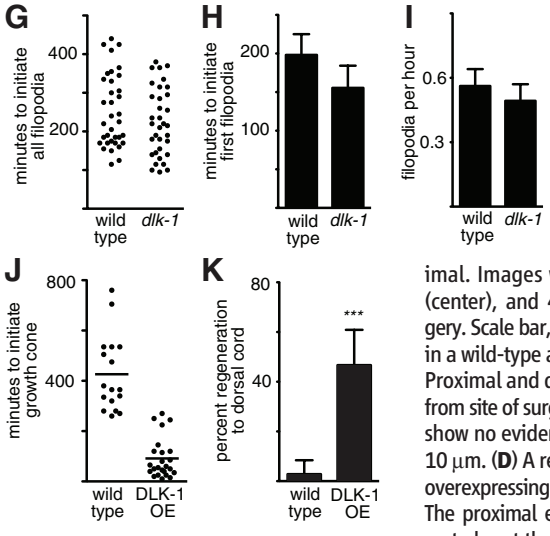

Fig. 3. *dlk-1* controls growth cone initiation and morphology during axon regeneration. (**A**) Transient filopodium in a wild-type animal. Images were taken at 165 (left), 170 (center), and 180 (right) minutes after surgery. Scale bar, 5 μm. (**B**) Transient filopodium in a *dlk-1* mutant animal. Images were taken at 475 (left), 480 (center), and 490 (right) minutes after surgery. Scale bar, 5 μm. (**C**) Representative axons in a wild-type animal 120 min after axotomy. Proximal and distal ends have retracted away from site of surgery, but proximal ends (arrows) show no evidence of regeneration. Scale bar, 10 μm. (**D**) A representative axon in an animal overexpressing DLK-1 120 min after axotomy. The proximal end (arrow) has already regenerated past the retracted distal end. Scale bar, 10 μm. (**E**) Representative growth cones in a wild-type animal. Although these axons successfully initiated regeneration, the growth cones (arrows) have a dystrophic morphology. Scale bar, 10 μm. (**F**) Representative growth cones in an animal overexpressing DLK-1 under the *unc-47* promoter. These growth cones (arrows) have a compact morphology similar to growth cones observed during development. Scale bar, 10 μm. (**G**) Distribution of all times of filopodia initiation in wild type and *dlk-1*. Each dot represents a filopodium. (**H**) Time of first filopodium initiation in wild type and *dlk-1*. Means ± SEM. (**I**) Rate of filopodia initiation in wild type and *dlk-1*. Means ± SEM. (**J**) Time to initiate regeneration after surgery in wild type and *dlk-1* overexpressing (OE) animals. Initiation is defined as the appearance of the filopodia that becomes a growth cone. Each dot represents a single axon. (**K**) Percentage of wild-type and *dlk-1* overexpressing (OE) regenerating axons that reached the dorsal cord after 18 to 24 hours. Error bars indicate 95% CI.

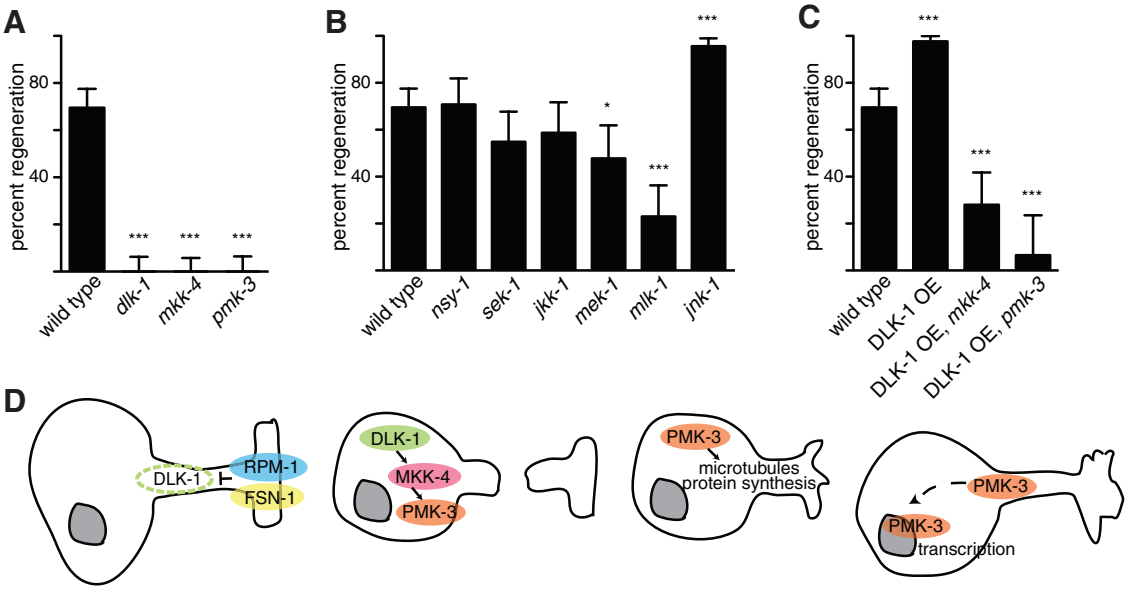

Fig. 4. MAP kinase signaling is required for axon regeneration. (**A**) Regeneration is eliminated by mutations in the DLK-1/MKK-4/PMK-3 MAP kinase module. (**B**) Other MAP kinase elements contribute to regeneration, but are not essential. (**C**) Activated DLK-1 has targets in addition to MKK-4 and PMK-3. (**D**) Model for function of MAP kinase signaling during axon regeneration. (A) to (C) Error bars indicate 95% CI.

defects in microtubule dynamics contribute to the axon outgrowth phenotype of *Phr1* mutant mice (*26*). Activated p38 may also control other targets that facilitate axon regeneration. p38 regulates local protein synthesis (*28*), which is required for regeneration (*19*). p38 is also likely to have functions in the nucleus, because it contributes to injury-induced changes in gene transcription (*29*). Activated p38 may reach the nucleus by retrograde transport. Retrograde transport in general is critical for regeneration (*30*), and transport of activated MAP kinases from axons to the cell body following axotomy has been observed in *Aplysia* sensory neurons (*31*) and in rodent sciatic nerves (*32*, *33*). Thus, regeneration may require activated PMK-3/p38 at the site of the break to regulate microtubule stability and protein expression and also may require PMK-3 to traffic to the nucleus to regulate gene transcription (Fig. 4D). The DLK-1 signaling pathway thus provides a critical link between axon injury and the process of regeneration.

References and Notes

1. L. C. Case, M. Tessier-Lavigne, *Curr. Biol.* **15**, R749 (2005).
2. F. Rossi, S. Gianola, L. Corvetti, *Prog. Neurobiol.* **81**, 1 (2007).
3. B. P. Liu, W. B. Cafferty, S. O. Budel, S. M. Strittmatter, *Philos. Trans. R. Soc. Lond. B Biol. Sci.* **361**, 1593 (2006).
4. S. Neumann, C. J. Woolf, *Neuron* **23**, 83 (1999).
5. M. Hammarlund, W. S. Davis, E. M. Jorgensen, *J. Cell Biol.* **149**, 931 (2000).
6. M. Hammarlund, E. M. Jorgensen, M. J. Bastiani, *J. Cell Biol.* **176**, 269 (2007).
7. K. Nakata *et al.*, *Cell* **120**, 407 (2005).
8. Materials and methods are available as supporting material on *Science* Online.
9. M. F. Yanik *et al.*, *Nature* **432**, 822 (2004).
10. Z. Wu *et al.*, *Proc. Natl. Acad. Sci. U.S.A.* **104**, 15132 (2007).
11. B. Grill *et al.*, *Neuron* **55**, 587 (2007).
12. D. Gitler, M. E. Spira, *J. Neurobiol.* **52**, 267 (2002).
13. S. Chierzi, G. M. Ratto, P. Verma, J. W. Fawcett, *Eur. J. Neurosci.* **21**, 2051 (2005).
14. S. Neumann, F. Bradke, M. Tessier-Lavigne, A. I. Basbaum, *Neuron* **34**, 885 (2002).
15. J. Qiu *et al.*, *Neuron* **34**, 895 (2002).
16. J. Silver, J. H. Miller, *Nat. Rev. Neurosci.* **5**, 146 (2004).
17. K. M. Knobel, E. M. Jorgensen, M. J. Bastiani, *Development* **126**, 4489 (1999).
18. C. V. Gabel, F. Antonie, C. F. Chuang, A. D. Samuel, C. Chang, *Development* **135**, 1129 (2008).
19. P. Verma *et al.*, *J. Neurosci.* **25**, 331 (2005).
20. J. J. Ewbank, *WormBook* (23 January 2006); doi/10.1895/wormbook.1.83.1, www.wormbook.org.
21. D. Nihalani, D. Meyer, S. Pajni, L. B. Holzman, *EMBO J.* **20**, 3447 (2001).
22. M. Mata, S. E. Merritt, G. Fan, G. G. Yu, L. B. Holzman, *J. Biol. Chem.* **271**, 16888 (1996).
23. A. Daviau *et al.*, *J. Biol. Chem.* **281**, 31467 (2006).
24. A. M. Schaefer, G. D. Hadwiger, M. L. Nonet, *Neuron* **26**, 345 (2000).
25. C. A. Collins, Y. P. Wairkar, S. L. Johnson, A. DiAntonio, *Neuron* **51**, 57 (2006).
26. J. W. Lewcock, N. Genoud, K. Lettieri, S. L. Pfaff, *Neuron* **56**, 604 (2007).
27. H. Erez *et al.*, *J. Cell Biol.* **176**, 497 (2007).
28. D. S. Campbell, C. E. Holt, *Neuron* **37**, 939 (2003).
29. H. Zrouri, C. Le Goascogne, W. W. Li, M. Pierre, F. Courtin, *Eur. J. Neurosci.* **20**, 1811 (2004).
30. S. Hanz, M. Fainzilber, *J. Neurochem.* **99**, 13 (2006).
31. Y. J. Sung, M. Povelones, R. T. Ambron, *J. Neurobiol.* **47**, 67 (2001).
32. E. Perlson *et al.*, *Neuron* **45**, 715 (2005).
33. A. J. Reynolds, I. A. Hendry, S. E. Bartlett, *Neuroscience* **105**, 761 (2001).

34. This work is dedicated to the memory of Craig H. Neilsen. We thank C.-B. Chen, D. Gard, W. Davis, J. White, and K. Schuske for helpful discussions. Supported by the Craig H. Neilsen Foundation, the McKnight Endowment Fund for Neuroscience, and NIH 1R21NS060275 to M.B. and NIH NS034307 to E.M.J.

Supporting Online Material

www.sciencemag.org/cgi/content/full/1165527/DC1
Materials and Methods
Table S1
References
Movie S1

4 September 2008; accepted 10 December 2008
Published online 22 January 2009;
10.1126/science.1165527
Include this information when citing this paper.

www.sciencemag.org/cgi/content/full/1165527/DC1

Supporting Online Material for

Axon Regeneration Requires a Conserved MAP Kinase Pathway

Marc Hammarlund, Paola Nix, Linda Hauth, Erik M. Jorgensen, Michael Bastiani*

*To whom correspondence should be addressed. E-mail: bastiani@bioscience.utah.edu

Published 22 January 2009 on *Science* Express
DOI: 10.1126/science.1165527

This PDF file includes

Other Supporting Online Material for this manuscript includes the following:
(available at www.sciencemag.org/cgi/content/full/1165527/DC1)

Materials and Methods

Strains

Animals were maintained on NG agar plates with *E. coli* HB101 as a food source according to standard methods. See Table S1 for all strains and complete genotypes. The wild type was EG1285 *oxIs12*.

RNAi

RNAi was performed by feeding as described (*S1*). Bleached embryos from MJB1046 *basIs1; oxIs268, unc-70(s1502); eri-1(mg366); lin-15(n765)* gravid hermaphrodites were placed on *dlk-1* RNAi bacteria. Plates were incubated at 15^{o}C for 12-13 days. A minimum of 10 F1 L4 animals were scored by counting all GABA commissures contacting the dorsal cord. Because commissures are sometimes obscured by other processes, this method slightly underestimates the actual number. For example, we typically scored 16 commissures in wild-type animals compared with the actual number of 19.

Axotomy

L4-stage hermaphrodites were mounted in 10 mM muscimol in M9 on an agarose pad under a cover slip. GFP-expressing DD and VD motor neurons were imaged with a Microradiance 2000 confocal microscope using a Nikon 60X, 1.4 NA lens. Selected commissural axons were cut using a 440-nm MicroPoint Laser System from Photonic Instruments. After surgery, animals were recovered to an agar plate, and remounted for confocal imaging approximately 18-24 hours post-surgery. The imaged commissures were classified according to the following criteria: 1) regeneration (number of commissures with well-defined growth cones present on the proximal fragment and/or a net growth of 5 μm or more, 2) sprouting (number of commissures with small branches present on the proximal fragment), and 3) no regeneration (no change to proximal fragment after 18-24 hours). A minimum of 20 individuals (with 1-3 axotomized commissures each) were observed for most experiments.

In cases where the genetic background resulted in improved regeneration the data are likely to be an underestimate of successful regeneration. To ensure that only axons which had been completely severed were analyzed, we eliminated experiments that did not include a growth cone and/or a recognizable distal fragment after 18-24 hours. This approach underestimates successful regeneration because any experiment in which the regenerated axon obscured the distal stump would appear as an uncut commissure and would be eliminated. 95% confidence intervals were calculated by the modified Wald method, and two-tailed P values were calculated using Fisher's exact test (http://www.graphpad.com/quickcalcs/).

Molecular Biology

Molecular biology was done using standard techniques. PCR was done with Phusion DNA Polymerase (Finnzymes). Templates were either genomic DNA from mixed-stage N2 or first strand cDNA obtained by dT-primed reverse transcription of poly-A selected RNA from mixed-stage N2. Plasmids were assembled using multisite Gateway recombination (Invitrogen).

pPN12 (Punc-47:dlk-1 minigene): A 5' fragment (exon 1 and 2) was amplified from genomic DNA and a 3' fragment (exons 3-11) from cDNA. The two fragments were ligated and a full-length product for generating a Gateway entry clone was obtained by amplifying with the following primers:

PN18 ggggacaagtttgtacaaaaaagcaggctggacatctaccacaatggtaacc
PN19 ggggaccactttgtacaagaaagctgggtgaattcggactgctccggcatcg.

The final construct was obtained in a multisite Gateway reaction using the following constructs: pMH522 (P*unc-47* [4-1]), pPN11 (*dlk-1* minigene [1-2]), pMH473 (*unc-54* terminator [2-3]), and pDEST [4-3].

pPN14 (Punc-47:dlk-1 cDNA-GFP): The genomic portion of pPN11 was replaced with a BstEII-SalI digested cDNA fragment (PN16 acatctaccacaatggtaacc, PN31 cggagcttcttctggcattg). The final construct was obtained in a multisite Gateway reaction using the following constructs: pMH522 (P*unc-47* [4-1]), pPN13 (*dlk-1* cDNA [1-2]), pGH50 (GFP:*unc-54* terminator [2-3]), and pDEST [4-3].

pMH524 (Phsp-16.2:dlk-1 cDNA-mCherry): The final construct was obtained in a multisite Gateway reaction using the following constructs: pMH520 (P*hsp-16.2* [4-1]), pPN13 (*dlk-1* cDNA [1-2]), pGH38 (mCherry:*unc-54* terminator [2-3]), and pCFJ150 MosSci [4-3].

Transgenics

Transgenic animals were obtained as described (*S2*). MJB1011 was constructed by injecting EG4529 *oxIs268* with pPN12 DNA at 30 ng/µl along with P*myo-2*:mCherry at 2 ng/µl as a co-injection marker. MJB1032 was constructed by injecting N2 with pPN14 DNA at 30 ng/µl along with P*unc-47*:mCherry at 20 ng/µl. EG5203 was constructed by injecting MJB1014 *dlk-1(ju476); oxIs12* with P*hsp-16-2*::DLK-1-mCherry at 5 ng/µl together with P*myo-2*::GFP at 2 ng/µl as an injection marker and 1 kb ladder at 50 ng/µl as carrier. Stable transgenic lines were recovered based on GFP in pharynx muscles and subjected to heat shock. Two out of three lines tested showed weak mCherry in the intestine 24 hours after heat shock, suggesting that heat shock resulted in appreciable expression of the DLK-1-mCherry fusion protein. One of these lines was used for further experiments.

Neuron Polarity

The L4-stage GABA motor neurons are of two types, DD and VD, with similar morphologies but opposite polarities (*S3*). Axotomy at the midline therefore severs the presynaptic region of the DD neurons and the postsynaptic region of the VD neurons. We typically cut VD11, VD10, and DD5. In some genetic backgrounds or developmental stages nearly all neurons regenerated; in others, such as *dlk-1* mutants, none did. Thus, as previously reported, regeneration was similar in DD and VD neurons (*S4*), and *dlk-1* is required in both neuron types. As an additional control we cut L1 stage identified DD axons, before VDs grew out, and compared their regeneration to identified VD axons cut during late L1. We observed no significant difference in DD regeneration compared with VD regeneration (Fig. 2E).

Development

To address a potential function for *dlk*-1 in development of the DD neurons, we imaged them in L1-stage animals, before they were masked by the VD neurons. We scored 100

L1 animals and found no difference from wild type in number of commissures, branching, path-finding errors, or other defects. We did observe a slight increase in gaps between dendrites along the dorsal cord. Although the number of gaps in the dorsal cord was not significantly different (P = 0.1757), there was a significant difference in average gap length, 2.3 um (range from 1 to 7 um) in the wild type and 4.4 um (range 1-10 um) in *dlk*-1 (P <0.0001).

Heat Shock

Mixed-stage animals were heat shocked at 33°C for 1 hour on a sealed worm plate in a recirculating water bath. L4-stage animals containing the P*hsp-16-2*::DLK-1-mCherry array were selected based on pharynx GFP.

Filopodia

Confocal images collected at 5-minute intervals were analyzed for the appearance of filopodia (small, transient extensions from the axon tip or shaft). Since some filopodia appear in only one frame, there are probably some even faster events that are too rapid to be captured by this imaging protocol. Thus, our data likely underestimate the true number of transient events. We analyzed 11 axons in 8 animals for wild type and 9 axons in 5 animals for *dlk-1(ju476)*. For wild-type axons, analysis was terminated at the appearance of the filopodium that eventually stabilized into a growth cone. The average time to this event was 460 minutes.

Since *dlk*-1 mutants never initiate growth cones, they continue to generate filopodia throughout the analysis, long after the average time to initiate a growth cone in wild type. Because these late events have no equivalent in wild-type animals, they were eliminated from the comparison in Figure 3G. Only events in both genotypes occurring before 460 minutes were considered. Figure 3H shows the average time and the standard error for the first event. Figure 3I shows the average rate. For this analysis, the number of filopodia observed in each axon was divided by the time of observation for that axon. Analysis was truncated at growth cone initiation or 460 minutes, whichever came first.

Time-lapse Microscopy

Methods are similar to those described (*S5*) with the following changes. L4 worms were anesthetized with 1 µl of 10 mM muscimol (Sigma M1523) in M9 and mounted on 5-10% agarose pads. Agarose included 0.002% 1-phenoxy-2-propanol (Janssen Chimica). Worms were cover slipped and the slide sealed in Vaseline to prevent evaporation. Axotomy was performed as described above, and time lapse images were collected (Lasersharp 2000) every 5 min over a Z range of 10-15 µm at 0.1 µm/pixel resolution. Maximum projections of each time point were exported to ImageJ for analysis.

References

S1. R. S. Kamath *et al.*, *Nature* **421**, 231 (2003).
S2. C. C. Mello, J. M. Kramer, D. Stinchcomb, V. Ambros, *EMBO J* **10**, 3959 (1991).
S3. J. G. White, E. Southgate, J. N. Thomson, S. Brenner, *Phil. Trans. Royal Soc. London* **314**, 1 (1986).
S4. Z. Wu *et al.*, *Proc Natl Acad Sci USA* (2007).
S5. K. M. Knobel, E. M. Jorgensen, M. J. Bastiani, *Development* **126**, 4489 (1999).

Hammarlund *et al*., Supplemental Table 1

	Genotype	Strain	# animals	# axons	# regeneration	P vs. control
wild type	*oxIs12*	EG1285	50	105	73 (70%)	
MAPKKK	*dlk-1(ju476); oxIs12*	MJB1014	24	69	0	<.0001
DLK-1 rescue	*dlk-1(ju476) basEx2*	MJB1032	21	53	43 (81%)	0.1314
RPM-1 OE	*basEx3; oxIs268*	MJB1034	22	43	3 (7%)	<.0001
E3 ligase	*rpm-1(ju41); oxIs12*	MJB1027	24	51	44 (86%)	0.0296
F-Box	*fsn-1(gk429); oxIs12*	MJB1025	24	65	56 (86%)	0.0163
Rab GTPase	*glo-1(zu391); oxIs268*	MJB1017	24	65	33 (51%)	0.0155
Rab GEF	*glo-4(ok623); oxIs12*	MJB1024	25	59	39 (66%)	0.7272
wt L1/2 DD	*oxIs12*	EG1285	16	17	15 (88%)	0.1484
wt L1/2 VD	*oxIs12*	EG1285	14	14	13 (93%)	0.1087
wt 2 day adult	*oxIs12*	EG1285	19	47	17 (36%)	<.0001
wt 5 day adult	*oxIs12*	EG1285	16	32	4 (13%)	<.0001
dlk-1 L1/2 DD	*dlk-1(ju476); oxIs12*	MJB1014	18	18	0	<.0001
dlk-1 2 day adult	*dlk-1(ju476); oxIs12*	MJB1014	20	38	0	<.0001
HS 0	*oxIs12*	EG1285	25	58	53 (91%)	0.0015
HS 0	*dlk-1(ju476); oxIs12*	MJB1014	20	57	0	<.0001
no HS	*dlk-1(ju476); oxIs12 oxEx1268*	EG5203	22	55	0	<.0001
HS-11	*dlk-1(ju476); oxIs12 oxEx1268*	EG5203	3	9	0	<.0001
HS -8	"	"	15	37	2 (5%)	<.0001
HS -4	"	"	10	23	8 (35%)	0.0034
HS -2	"	"	7	17	7 (41%)	0.0292
HS 0	"	"	13	25	21 (84%)	0.2135
HS +2	"	"	10	24	10 (42%)	0.0169
HS +4	"	"	17	46	23 (50%)	0.0276
HS +8	"	"	14	34	13 (38%)	0.002
HS +24	"	"	22	60	8 (13%)	<.0001
HS +48	"	"	35	96	1 (1%)	<.0001
HS +48 L2	"	"	16	16	0	<.0001
MAPKK	*mkk-4(ju91); oxIs268*	MJB1015	31	76	0	<.0001
MAPK	*pmk-3(ok169); oxIs12*	MJB1013	22	69	0	<.0001
MAPKKK	*nsy-1(ok593); oxIs12*	MJB1026	21	48	34 (71%)	1
MAPKK	*sek-1(km4); oxIs268*	MJB1022	23	51	28 (56%)	0.0777
MAPKK	*jkk-1(km2); oxIs268*	MJB1021	24	46	27 (59%)	0.2618
MAPKKK	*mlk-1(ok2471); oxIs12*	MJB1029	24	52	12 (23%)	<.0001
MAPKK	*mek-1(ks54); oxIs268*	MJB1020	21	46	22 (48%)	0.0168
MAPK	*jnk-1(gk7); oxIs12*	MJB1023	27	68	65 (96%)	<.0001
DLK-1 OE L4	*basEx1; oxIs268*	MJB1011	22	43	42 (98%)	<.0001
DLK-1 OE 5 day adult	*basEx1; oxIs268*	MJB1011	27	53	38 (72%)	0.8548
DLK-1 OE, *mkk-4*	*mkk-4(ju91); basEx1; oxIs268*	MJB1038	24	50	14 (28%)	<.0001
DLK-1 OE, *pmk-3*	*pmk-3(ok169); basEx1; oxIs268*	MJB1039	25	46	3 (7%)	<.0001

Transgenes	Allele	Contents
GFP	*oxIs12 X*	P*unc-47*:GFP, *lin-15*(+)
GFP	*oxIs268 III*	P*unc-47*:GFP
DLK-1 rescue	*basEx2*	P*unc-47*:DLK-1 cDNA-GFP; P*unc-47*:mCherry; P*myo-2*:mCherry
DLK-1 HS	*oxEx1268*	P*hsp-16.2*:DLK-1 cDNA, P*myo-2*:GFP
DLK-1 OE	*basEx1*	P*unc-47*:DLK-1 minigene, P*myo-2*:mCherry
RPM-1 OE	*basEx3*	P*unc-25*:RPM-1 genomic (pCZ480—gift of Yishi Jin), P*myo-2*:mCherry

All P values are two-tailed and are calculated against the L4 wild type (EG1285 *oxIs12*, top row of this table) using Fisher's exact test (http://www.graphpad.com/quickcalcs/contingency1.cfm).